Joint Effects of Heat Stress and $PM_{2.5}$ Exposure on Glucose Metabolism and Hepatic Insulin Signaling

Weijia Gu
Zhejiang Chinese Medical University https://orcid.org/0000-0003-2613-0981
Ziwei Cai
Zhejiang Chinese Medical University
Mianhua Zhong
New York University
Lung-Chi Chen
New York University
Lu Zhang
Zhejiang Chinese Medical University
Xiujuan Lin
Zhejiang Chinese Medical University
Rucheng Chen
Zhejiang Chinese Medical University
Ran Li
Zhejiang Chinese Medical University
Li Qin
Zhejiang Chinese Medical University
Qinghua Sun
The Ohio State University
Cuiqing Liu (liucuiqing@zcmu.edu.cn)
School of Basic Medical Sciences and Public Health, Joint China-US Research Center for Environment and Pulmonary Diseases, Zhejiang Chinese Medical University, Hangzhou 310053, China

Research

Keywords: Heat stress, Fine particulate matter, Insulin resistance, HSP72

Posted Date: June 30th, 2021

DOI: https://doi.org/10.21203/rs.3.rs-659151/v1

Abstract

Background: Heatwave events are occurring more frequently, accompanied by a significant increase in the ambient concentration of fine particulate matter ($PM_{2.5}$). Epidemiological studies have suggested that heat stress or $PM_{2.5}$ exposure would impair glucose homeostasis and insulin sensitivity, but the combined effect and the exact mechanisms are not well understood.

Methods: C57BL/6 mice were randomly divided into filtered air (FA), fine particulate matter (PM) group, filtered air combined with heat stress (FH) group, and fine particulate matter combined with heat stress (PH) group for a 4-week $PM_{2.5}$ exposure, followed by a 2-week heat stress exposure, via a whole-body exposure system. Systemic glucose homeostasis, insulin sensitivity, and circulating inflammatory cytokines were examined. HSP72 expression and insulin signaling in the liver were measured.

Results: Glucose tolerance and insulin sensitivity were impaired in response to heat stress, accompanied by lessened hepatic GLUT2 expression and inhibited insulin signaling pathway. No synergistic effects of heat stress and $PM_{2.5}$ exposure on glucose homeostasis were observed, while heat-upregulated HSP72 expression was attenuated with accumulated TNF-α induced by further $PM_{2.5}$ exposure.

Conclusions: Heat stress combined with $PM_{2.5}$ exposure induced TNF-α, which could inhibit heat-elevated hepatic HSP72 expression. Elevated circulating TNF-α impaired hepatic insulin signaling and GLUT2 expression. Then, glucose homeostasis was perturbed, and insulin action was impaired.

Background

According to the European Copernicus Climate Change Service, the average temperature in Europe in 2019 was about 1.2°C higher than the average temperature in the past 40 years, which was the hottest year on record[1] . China's climate warming in the past 60 years has been particularly pronounced, with an average increase of about 0.23°C every 10 years, almost twice of the global rate [2]. There is increasing evidence that both mortality and morbidity increased as temperature rose, especially in elderly people with pre-existing conditions of cardiovascular, cerebrovascular, and respiratory diseases [3, 4]. Based on an estimate of 831 million urban residents in China, every 0.5°C increase in surface temperature from the current level will result in more than 27,900 heat-related deaths each year [5]. These extreme weather episodes not only impact human health, but also influence a variety of other global changes (e.g., population growth, urbanization, land use changes, and natural resource depletion) and potentially augment their impacts [6].

Although some critical issues of climate change remain unresolved, it is generally believed that this is mainly due to the increase in greenhouse gas emissions [7]. There is an inherent link between climate change and air pollution because greenhouse gases and air pollutants come from similar or even the same sources, such as fossil fuel combustion, which is the main source of both greenhouse gases (CH_4, CO_2) and criteria air pollutants (particulate matter [PM], CO, SO_X, NO_X) [8]. During a heatwave, elevated

temperature is characteristically accompanied by corresponding increases in the concentrations of air pollutants, such as PM and O_3 [9]. To date, no animal study has examined the simultaneous effects of temperature and PM exposure. Although another air pollutant, O_3, has also been shown to interact with heat stress, most of the increased risk is on the pulmonary system [10]. Therefore, increases in mortality or morbidity may feasibly be attributed to an interaction between heat and air pollutant factors. Recent studies have shown that both PM pollution and temperature change are associated with adverse health outcomes [11, 12], and PM leads to the largest effect on mortality on hot days [13]. In China, the risk of total mortality, cardiovascular mortality, and respiratory mortality per 10 μg/m^3 increment in PM_{10} increased more than 2-fold on high temperature days [14]. Importantly, one study suggested that the threshold of different pollutants, above which these effects become measurable, appears to be lowered during extremely hot days [15]. Therefore, it is likely that the true magnitude of the interactions between high temperature and PM pollution is underestimated. We hypothesized that heat stress combined with $PM_{2.5}$ exposure would impair glucose homeostasis and insulin sensitivity. The combined effects of PM and high temperature need to be considered and investigated to establish adequate public health policies and actions to face anticipated future changes in air quality and climate. It is widely accepted that respiratory system response during PM exposure involves inflammatory pathways [16]. Severe heat stress also leads to features of proinflammatory cytokines (e.g., IL-1β, tumor necrosis factor (TNF)-α) and hepatic oxidative stress (e.g., lipid peroxidation, glutathione oxidation) [17]. During exercises in a hot and humid environment, tissue damage was found particularly in liver that was related to inflammation, oxidative stress, and apoptosis [18]. Liver injury is a common complication of heat stress, which has been proved to be mediated by IL-1β [19]. In turn, excessive inflammatory cytokines could inhibit the production of heat shock proteins (HSP)72 [20]. In addition to cytokines, up-regulation of HSP is one of the primary cellular defense mechanisms against heat stress [21]. Studies showed that HSP72 and HSP90 were significantly higher in heat intolerant mice following heat exposure compared to heat tolerant mice [22]. Interestingly, these findings suggest a substantial overlap in the mechanisms of metabolism and inflammation, which underlie progressive insulin resistance and peripheral inflammation [23]. Our previous studies revealed that $PM_{2.5}$ exposure significantly reduced insulin sensitivity in the liver [24, 25] and disrupted the rhythms of key enzymes involved in hepatic lipid metabolism [26]. These evidences suggest that liver is an important target organ for $PM_{2.5}$ exposure.

Considering that heat stress and $PM_{2.5}$ exposure may work on the same/close targets, we therefore were particularly interested in the interactive effects of heat stress and “real world” ambient $PM_{2.5}$ exposure on liver metabolism. In this study, we systematically investigated this issue in C57BL/6 mice subjected to heat stress combined with $PM_{2.5}$ exposure.

Methods

Reagents and antibodies

Human regular insulin (Humulin) was purchased from Lilly (Indianapolis, IN, USA). Mouse inflammation Cytometric Bead Array (CBA) kits (Catalog No. 552364) were obtained from BD Biosciences (San Jose, CA, USA). Alexa Fluor 488-conjugated goat anti-Rabbit IgG secondary antibody (1:200) was purchased from Thermo Fisher Scientific (Carlsbad, CA, USA). Antifade mounting medium with (4',6-diamidino-2-phenylindole) DAPI, RIPA lysis buffer, protease inhibitors, and Pierce BCA Protein Assay kit were purchased from Beyotime (Shanghai, China). Immun-Star HRP Substrate (1705041) was purchased from Bio-Rad Laboratories, Inc. (Hercules, CA, USA). RNAiso Plus was obtained from Takara Biomedical Technology (Beijing, China). Phosphatase inhibitors were purchased from Roche (Basel, Switzerland). Rabbit anti-mouse antibody for GLUT2 (ab54460) was bought from Abcam Inc. (Cambridge, MA, USA). Rabbit anti-mouse antibodies for HSP72 (#4872), IRS-1 (#2382) and phosphorylated (p)-IRS-1 (Ser307) (#2381), Akt (#9272) and phosphorylated (p)-Akt (Ser473) (#4060) were obtained from Cell Signaling Technology (Danvers, MA, USA). Rabbit anti-mouse antibody for GAPDH (60004-1) was bought from Proteintech Group, Inc (Wuhan, China). Goat anti-rabbit horseradish peroxidase (HRP) conjugated secondary antibody (GAR0072) was bought from Multi Sciences Boitech (Hangzhou, China).

Animals and animal care

Male C57BL/6 mice (8-10 weeks) were purchased from Shanghai Laboratory Animal Co., Ltd. (Shanghai, China). All experiments and surgical procedures were approved by the Animal Care and Use Committee of Zhejiang Chinese Medical University with an animal use grant number of SYXK (Zhe) 2021-0012. All mice were maintained at 21 ± 1°C on a 12 h light/dark cycle, with ad libitum access to food and water. After heat stress combined with $PM_{2.5}$ inhalational exposure, all mice were anesthetized using 1.5% isoflurane and laid supine on a platform. Blood samples were collected from heart cavities and mice livers were harvested.

Heat stress combined with ambient whole-body $PM_{2.5}$ inhalational exposure protocol

All mice were randomly divided into 4 groups (filtered air [FA] group, fine particulate matter [PM] group, filtered air combined with heat stress [FH] group, and fine particulate matter combined with heat stress [PH] group). Two weeks before ambient whole-body $PM_{2.5}$ inhalational protocol, 5 mice in each group were randomly selected, and telemetry sensors (DSI, ETA-F20) were implanted into abdominal cavity by surgery under anesthesia [27]. One week after the surgery, all mice were subjected to either filtered air (FA) or ambient $PM_{2.5}$ for 6 h/d, 5 d/week from April 23, 2019 to June 4, 2019, for a total duration of 6 weeks, in a set of exposure system of “Zhejiang Whole-body Exposure System 1” located on the campus of Zhejiang Chinese Medical University in Hangzhou [25]. The system consists of four temperature-controlled chambers. The ambient air is connected to PM chambers, in which the particles larger than 2.5 μm are removed by cyclone separator and evenly distributed in the PM chambers. The FA chambers are equipped with HEPA filter in the inlet valve to remove all the $PM_{2.5}$ in the air stream. All mice were housed in separated cages with 3-4 mice/cage in each chamber. The temperature of the heat stress chambers was raised to 37 ± 0.2°C gradually within an hour period [28, 29]. A core temperature of 37°C is below the temperature (42.4°C) that has been considered as a mild heat stress [28, 29] and has been shown to

produce minimal pathological changes in the lungs and brain [30]. Temperature and humidity in the inhalation chambers were monitored continuously (Sup. 1 A and B). Mice are nocturnal and will be exposed to $PM_{2.5}$ and heat stress during their active period. Because air pollution levels are generally lower at night as compared to the daytime period, we need to reverse the animals' circadian cycle. Right after the 4^{th} week of the ambient whole-body $PM_{2.5}$ inhalation, temperature in the chamber of FH and PH was set to 37°C from 10:00 to 13:00 (3 hours) every other day (for a total of 4 days). During the 6^{th} week of the ambient whole-body $PM_{2.5}$ inhalation, temperature in the chamber of groups FH and PH was set to 37°C from 22:00 to 1:00 (3 hours) every other day (for a total of 4 days) (Fig. 1A). Monitoring of the FA and PM exposure environments within the two chambers was continuously recorded with an Aerosol Monitoring Meter (pDR-1500, Thermal Scientific, China), which was zero-adjusted before use. The data of environmental ambient aerosol concentration were collected from an adjacent local EPA monitoring station, which was located at the intersection of Jiangnan Ave. and Jiangling Rd., 10 km away from the study site. The temperatures of experimental mice and 4 chambers were acquired by DSI telemetry system, which were collected and recorded every 5 minutes throughout the experiment.

Sampling and analysis of $PM_{2.5}$ in the exposure chambers

To calculate $PM_{2.5}$ mass concentrations in the exposure chambers, $PM_{2.5}$ samples in the exposure chambers were collected on Teflon filter membranes (Teflon, 37 mm, 2 μm pore; GE healthcare, Amersham Place, UK). Teflon filter membranes from PM chamber were collected daily, while the filter membranes from FA chamber were collected weekly. A microbalance (Excellence Plus XP, Mettler Toledo, Switzerland) was used to weigh the membrane before and after sampling in a climate-controlled weighing chamber. Weight gains were used to calculate the exposed concentrations in the chambers. Analyses for major elements (Na, Mg, Si, S, K, Ca, Ti, Mn, Fe, Ni, Cu, Zn, Sr, Y) were performed using inductively coupled plasma mass spectrometry (ICP-MS, Thermo Fisher Scientific, Bremen, Germany).

Measurements of blood glucose homeostasis and insulin sensitivity

Glucose tolerance test (GTT) was conducted right after the heat stress combined with $PM_{2.5}$ exposure. Mice were fasted overnight (16 hours) and intraperitoneally injected with dextrose (2 mg/g body weight). Blood samples were collected from vena caudalis and blood glucose was measured by a FreeStyle blood glucose meter (Abbott Diabetes Care Inc., Alameda, CA, USA) at baseline, and 30, 60, 90, and 120 min after the dextrose injection. Three days after GTT, insulin sensitivity was measured by insulin tolerance test (ITT) via human regular insulin (0.5 U/kg body weight) injected intraperitoneally after 4.5 h fasting. At baseline and 30, 60, 90 and 120 minutes after insulin injection, blood glucose was measured by the same type of blood glucose meter in the same way as GTT.

Measurement of blood inflammatory biomarkers

Circulating cytokine levels were measured by CBA kit. Plasma was incubated with beads specific for TNF-α and IL-6 according to manufacturer's instructions. The total amount of cytokines was then determined

using a BD Accuri C6 Plus instrument and analyzed by BD FCAP Array Software v3.0 (BD Biosciences, San Jose, CA, USA).

Immunofluorescence analysis

After the exposures, liver segments were preserved via intracardiac perfusion with 30-40 ml of normal saline containing 0.02% heparin, followed by 30-40 ml of 4% paraformaldehyde in 0.1 M potassium phosphate buffer (pH = 7.4) when mouse was under anesthesia. Fixed liver tissue was embedded in paraffin and sectioned into 5-μm-thick. After deparaffinization in xylene for 10 min followed by 100% ethanol, slices were washed three times in phosphate-buffered saline (PBS). Nonspecific binding was blocked with 10% normal goat serum at room temperature for 30 min. An overnight incubation with rabbit anti-GLUT2 antibody (1:200) at 4°C was followed by 2 h of incubation with Alexa Fluor 488-conjugated goat anti-rabbit-lgG secondary antibody (1:200) at room temperature. The slices were washed and incubated with antifade mounting medium with DAPI as a nuclear stain. Finally, the slides were observed under a Leica fluorescence microscope DM4 B (Leica Microsystems, Wetzlar, Germany).

Total protein extraction and Western blotting analysis

Liver tissue was homogenized in 250 μL of cold RIPA lysis buffer with protease inhibitors and phosphatase inhibitors to obtain total protein for 30 min and then centrifuged at 12,000 ×g for 10 min at 4 °C. Supernatants assayed for protein using a Pierce BCA Protein Assay Kit and quantified to same concentration of protein (3 μg/μL). Equal amounts of proteins were loaded onto 8%-12% SDS-polyacrylamide gel, which was transferred to polyvinylidene fluoride membranes after electrophoresis. After blocking the nonspecific sites, the membranes were incubated at 4°C overnight. The following primary antibodies were used in this experiment: anti-HSP72, anti-IRS-1, anti-p-IRS-1 (Ser307), anti-Akt, anti-p-Akt (Ser473), anti-GLUT2 and anti-GAPDH. The membranes were probed with a goat anti-rabbit HRP-conjugated secondary antibody at room temperature for an hour. ChemiDoc Touch ImagingSystem (Bio-Rad Laboratories, Inc. Hercules, CA, USA) was used to detect protein bands. Band densities were normalized to GAPDH in each sample.

Measurement of gene expression by real-time RT-PCR

RT-PCR was performed using RNA extracted from mouse liver tissue. Total RNA was isolated with RNAiso Plus according to the manufacturer's protocol. It was then converted to cDNA using High-Capacity cDNA Reverse Transcription Kit (Applied Biosystems, Carlsbad, California, USA) and analyzed by RT-PCR on QuantStudio 6 Flex system using SYBR Green (ThermoFisher, Waltham, MA, USA). The expression level for each gene was calculated using the ΔCt method relative to β-actin. The sequences of all primers used are listed in Table 1.

Statistical nalysis

All data were analyzed with Prism v.8.3.0 (GraphPad Inc., USA). Results are expressed as mean ± standard error of mean (SEM) unless notified otherwise. P values of less than 0.05 were considered

statistically significant. Statistically significant values were compared using a two-way ANOVA followed by bonferroni's multiple comparisons test.

Results

$PM_{2.5}$ exposure characterization

The exposure period covered seasons of spring and summer in 2019. Correlation was observed with $PM_{2.5}$ levels in the PM chamber and the ambient air from the monitoring station. The regression coefficient between exposure chamber and ambient air concentrations was 0.399 (P = 0.009). The maximum and minimum values in the FA chamber were 2.47 μg/m^3 and 1.24 μg/m^3, respectively, with the mean concentration 1.49 ± 0.08 μg/m^3. The maximum and minimum values in the ambient air were 59 μg/m^3 and 10 μg/m^3, respectively, with the mean concentration 35.51 ± 1.96 μg/m^3. The maximum and minimum values of $PM_{2.5}$ levels in the PM chamber were 150.63 μg/m^3 and 17.83 μg/m^3, respectively, with the mean concentration 66.61 ± 4.16 μg/m^3 (1.88-fold concentration from ambient $PM_{2.5}$ level) (Fig. 1, B and C). Elemental composition of $PM_{2.5}$ at the study site was demonstrated in Table 2.

Metabolic characteristics of heat stress combined with $PM_{2.5}$ exposure in mice

Six weeks of $PM_{2.5}$ or heat stress exposure resulted in no differences in the body weights or average food intake among the four groups (Fig. 2, A and B). Right after the heat stress combined with $PM_{2.5}$ exposure, GTT was performed. Three days after GTT, ITT was measured. Compared with the FA group, heat stress significantly elevated blood glucose levels in FH mice at 30- and 60-min during GTT (Fig. 2C). Compared with the PM group, heat stress combined with $PM_{2.5}$ exposure demonstrated significant elevation of blood glucose levels in PH mice at 30-min during GTT (Fig. 2C). Compared with the FA group, heat stress combined with $PM_{2.5}$ exposure significantly elevated blood glucose levels in FH mice at 30- and 60-min during GTT (Fig. 2C). Compared with the FA group, heat stress impaired insulin sensitivity in FH mice at 90-min during ITT (Fig. 2E). Compared with the PM group, heat stress combined with $PM_{2.5}$ exposure also significantly impaired insulin sensitivity in PH mice at 60-, 90-, and 120-min during ITT (Fig. 2E). Compared with the FA group, heat stress combined with $PM_{2.5}$ impaired insulin sensitivity in FH mice at 90- and 120-min during ITT (Fig. 2E). However, compared with FH group, heat stress combined with $PM_{2.5}$ exposure induced no further impairment in GTT or ITT (Fig. 2, C and E). Area under the curves (AUC) analysis of GTT and ITT confirmed these findings (Fig. 2, D and F). These results indicated that heat stress or heat stress combined with $PM_{2.5}$ exposure, but not $PM_{2.5}$ exposure alone, impaired glucose homeostasis and insulin sensitivity.

Heat stress combined with $PM_{2.5}$ exposure elevated circulating TNF-α and decreased expression of HSP72 in the liver

To comprehensively understand the effects of heat stress and $PM_{2.5}$ on organ inflammation, hepatic pro-inflammatory cytokine production was examined with RT-PCR and Cytometric Bead Array kit. After 6 weeks of exposure, although there was no significant difference in the expression pattern of *IL-1β*, *IL-6*, or *TNF-α* among the four groups, the PM and FH mice exhibited a light increase in mRNA and circulating levels of IL-6 and TNF-α (Fig. 3A). Interestingly, compared with PM mice or FA mice, the circulating level of TNF-α was significantly higher in PH mice. Although no significant increase was shown, the circulating levels of TNF-α was about 63.7% higher in PH mice than that in FH mice (Fig. 3B). As shown in Fig 3C, heat stress alone induced significant increase in HSF72 in the liver, while significant downregulation in HSP72 was observed between FH and PH mice. Furthermore, heat stress combined with $PM_{2.5}$ exposure resulted in no difference in the amount of HSP72 protein compared with $PM_{2.5}$ exposure (Fig. 3C). We further investigated the HSF1/HSPA1A axis (critical for the transcription of HSP72) in the liver by RT-PCR. The levels of *HSF1* mRNA and *Hspa1a* mRNA showed no differences among groups (Fig. 3D). Marked histologic structural damages were observed in FH and PH mice, while normal light microscope appearance was better preserved in FA and PM mice (Sup. 2).

Heat stress combined with $PM_{2.5}$ exposure attenuated hepatic GLUT2 protein expression and insulin signaling.

As shown in Fig. 4A, hepatic GLUT2 expression was examined with immunofluorescence assay. Quantitative analysis of MFI (mean fluorescence intensity) indicated that the expression of hepatic GLUT2 was attenuated by $PM_{2.5}$, heat stress, or heat stress combined with $PM_{2.5}$ exposure (Fig. 4B). Similar inhibition on GLUT2 expression was observed at protein level (Fig. 4C). To further confirm the effects of heat stress or $PM_{2.5}$ exposure, *Slc2a2* (transcription factor for GLUT2) was examined by RT-PCR. Although no significant alteration in response to $PM_{2.5}$ exposure, PM mice showed a trend toward downregulation of *Slc2a2* in the liver compared to FA. Furthermore, both FH and PH mice exhibited significant decrease in its mRNA expression (Fig. 4D). To further confirm the inhibitory effect of heat stress and/or $PM_{2.5}$ exposure on hepatic insulin signaling, phosphorylated levels of IRS-1 at Ser307 were further examined. Compared to FA group, heat stress exposure significantly elevated the level of p-IRS-1^{Ser307}. It was the same case when heat stress combined with $PM_{2.5}$ exposure compared to the PM group ($P = 0.05$) (Fig. 4E). Akt is the activated downstream of the IRS family, which is necessary for GLUT2 function [31, 32]. To further confirm the effects of heat stress and/or $PM_{2.5}$ exposure, phosphorylated levels of Akt at Ser473 were examined. Compared to FA group, p-Akt^{Ser473} was significantly inhibited in response to heat stress or heat stress combined with $PM_{2.5}$ exposure. However, there was no statistical difference at the phosphorylated levels of Akt between FA and PM mice, FH and PH mice (Fig. 4F).

Discussion

The adverse health effects of heat stress combined with $PM_{2.5}$ exposure, which is demonstrated with epidemiological studies, has not been investigated in animal studies. In the present study, we used C57BL/6 mice to investigate the impact of heat stress combined with $PM_{2.5}$ exposure on insulin signaling

in the liver. Our major findings include: a) Impaired glucose tolerance and insulin sensitivity in response to heat stress; b) Inhibited hepatic GLUT2 expression mediated by insulin signaling due to heat stress; c) No synergistic effects of heat stress and $PM_{2.5}$ exposure on glucose homeostasis.

HSP72 is a major stress-inducible chaperone protein, which folds newly translated and misfolded proteins correctly and stabilizes or degrades mutant proteins [33]. Overexpression of HSP72 protects cells from stresses, including heat stress and oxidative stress [34]. Recent clinical and experimental evidences suggest a complex interaction between heat stress and systemic inflammatory response syndrome, of which cytokines have been implicated as adverse mediators [35]. Consistent with it, the protective expression of HSP72 in the liver and the circulating level of TNF-α were upregulated by heat stress exposure in the present study. However, despite of significantly increased circulating TNF-α, hepatic expression of HSP72 decreased in presence of heat stress combined with $PM_{2.5}$ exposure. Studies have shown that excessive expression of inflammatory factor TNF-α could inhibit the HSF1/HSPA1A axis, which is critical for the transcription of HSP72 [36, 37]. Thus, protective upregulation of HSP72 induced by heat could be offset by $PM_{2.5}$ exposure plus heat stress-enhanced TNF-α secretion. However, the exact mechanism and the interaction between TNF-α and HSP72 under heatwaves, merits further investigation.

Previous studies have clearly shown that insulin sensitivity could be improved by HSP72 induction via heat treatment (42°C for 30 min), pharmacologic intervention, and transgenic overexpression [23, 38, 39]. On the other hand, mice with HSP72 deletion were prone to be obese and glucose intolerant [40], further supporting the role of HSP72 in metabolic regulation. However, something contrary between HSP72 and glucose metabolic disorder was observed. In addition to systemic insulin sensitivity, the molecules in hepatic insulin signaling pathway were also explored. GLUT2 expression is critical for the control of glucose-sensitive genes, and inactivation of GLUT2 in the liver impaired glucose-stimulated insulin secretion [41]. GLUT2 expression was significantly inhibited by heat stress or heat stress combined with $PM_{2.5}$ exposure, which was regulated by its transcription factor *Slc2a2*. The alteration of GLUT2 levels were mostly in line with the changes of p-IRS-1^{Ser307} and p-Akt^{Ser473}, downstream of classic insulin signaling pathway [42]. Thus, heat stress itself may impair hepatic insulin signaling and GLUT2 expression, which interfered glucose transport to hepatocytes and resulted in the elevation of blood glucose in GTT and ITT. We noticed that the changes of hepatic GLUT2 were inconsistent with the results of GTT and ITT measurements, particularly for PM mice. The ITT and GTT are mainly affected by three key insulin target tissues: skeletal muscle, liver, and white adipose tissue [43]. Our previous study found that exposure to $PM_{2.5}$ significantly reduced the insulin sensitivity of the three key insulin target tissues, but the sensitivity of each tissue was quite different [44]. Excessive inflammatory cytokines have been shown to impair insulin sensitivity [45, 46] and inhibit the production of HSP72 [20] as well. The failure of HSP72 to protect insulin sensitivity may be due to the offset of insulin sensitivity by heat- or heat plus $PM_{2.5}$ exposure-induced TNF-α secretion and direct inhibition of inflammation on HSP72 expression itself.

Different from our previous studies, we found no impairment in glucose homeostasis and insulin sensitivity in $PM_{2.5}$ exposed mice [24, 26]. We suppose that it may be due to insufficient $PM_{2.5}$ exposure duration (6-week duration) [44, 47]. Even though, inhibited GLUT2 expression and a trend toward decrease in p-Akt^{Ser473} was shown, indicating the presence of $PM_{2.5}$ exposure induced adverse effects. Our component analysis showed that metals and inorganic ions were the most abundant components in $PM_{2.5}$ samples. Researchers also pointed out that $PM_{2.5}$-bound metal could affect not only the respiratory system but also metabolism (hepatic urea synthesis and fat deposits) [48, 49]. It makes us to speculate that the toxic effect of $PM_{2.5}$ under current situation (concentration and components) may be not so strong as that in previous studies. Although epidemiological survey demonstrated that PM concentration increased simultaneously during a heatwave [9], no further toxic effects of $PM_{2.5}$ exposure upon heat stimulation were observed. The trend toward increase in circulation TNF-α and attenuation of hepatic HSP72 expression indicated the presence of, albeit little, interactive action in response to heat stress combined with $PM_{2.5}$ exposure. Thus, the exact adverse effects of multiple environmental factor exposure await further investigations with more sophisticated designs.

Conclusions

In summary, our data showed that heat stress combined with $PM_{2.5}$ exposure induced TNF-α, which could inhibit heat-elevated hepatic HSP72 expression. Elevated circulating TNF-α impaired hepatic insulin signaling and GLUT2 expression. Then, glucose homeostasis was perturbed, and insulin action was impaired. The above results provide a new perspective for revealing the etiology of liver metabolism abnormality from the viewpoint of insulin resistance induced by heat stress combined with $PM_{2.5}$.

Abbreviations

CBA: Cytometric Bead Array; FA: Filtered Air; FH: Filtered Air Combined with Heat Stress; $PM_{2.5}$: Fine Particulate Matter; PH: Fine Particulate Matter Combined with Heat Stress; GTT: Glucose Tolerance Test; HSP72: Heat Shock Protein 72; HRP: Horseradish Peroxidase; Humulin: Human Regular Insulin; ITT: Insulin Tolerance Test; MFI: Mean Fluorescence Intensity; PBS: Phosphate-Buffered Saline; SEM: Standard Error of Mean; TNF-α: tumor necrosis factor-α

Declarations

Ethics approval and consent to participate

Animal experiments were in accordance with the National Institute of Health Guide for the Care and Use of Laboratory Animals, with the approval of the Animal Care and Use Committee at Zhejiang Chinese Medical University.

Consent for publication

Not applicable.

Availability of data and materials

All the relevant data and materials are presented in this article.

Competing interests

The authors declare that they have no competing interests.

Funding

This work was supported by National Natural Science Foundation of China (grant number: 81904027 and 81973001), Medical Health Science and Technology Project of Zhejiang Provincial Health Commission (grant number: 2019KY471 and 2019KY472), Natural Science Foundation of Zhejiang Chinese Medical University (grant number: KC201901 and 2019ZR02), and Key R&D International Cooperation Projects (grant number: 2019YFE0114500).

Authors' contributions

Weijia Gu, Ziwei Cai, Mianhua Zhong, Lu Zhang, Xiujuan Lin, Rucheng Chen, Ran Li, and Li Qin performed the experiments and generated data. Mianhua Zhong and Lu Zhang helped with data collection and analysis. Lung-Chi Chen and Qinghua Sun helped with manuscript edition. Lung-Chi Chen and Weijia Gu designed the experiments. Weijia Gu and Cuiqing Liu drafted the manuscript. Cuiqing Liu is the guarantor of this work, had full access to all the data, and takes full responsibility for the integrity of data and the accuracy of data analysis. The author(s) read and approved the final manuscript.

Acknowledgements

Not applicable.

Authors' information

[1] School of Basic Medical Sciences and Public Health, Joint China-US Research Center for Environment and Pulmonary Diseases, Zhejiang Chinese Medical University, Hangzhou 310053, China

[2] Department of Environmental Medicine, New York University School of Medicine, New York, USA.

[3] College of Public Health, The Ohio State University, Columbus, OH, USA

References

1. Blunden J, Arndt DS. State of the Climate in 2019. Bulletin of the American Meteorological Society. 2020;101(8):S1-S429.

2. Cavicchioli R, Ripple WJ, Timmis KN, Azam F, Bakken LR, Baylis M, et al. Scientists' warning to humanity: microorganisms and climate change. Nat Rev Microbiol. 2019;17(9):569-86.

3. Ye X, Wolff R, Yu W, Vaneckova P, Pan X, Tong S. Ambient temperature and morbidity: a review of epidemiological evidence. Environ Health Perspect. 2012;120(1):19-28.

4. De Sario M, Katsouyanni K, Michelozzi P. Climate change, extreme weather events, air pollution and respiratory health in Europe. Eur Respir J. 2013;42(3):826-43.

5. Wang Y, Wang A, Zhai J, Tao H, Jiang T, Su B, et al. Tens of thousands additional deaths annually in cities of China between 1.5 °C and 2.0 °C warming. Nat Commun. 2019;10(1):3376.

6. Hylander BL, Gordon CJ, Repasky EA. Manipulation of Ambient Housing Temperature To Study the Impact of Chronic Stress on Immunity and Cancer in Mice. J Immunol. 2019;202(3):631-6.

7. Change IC. The physical science basis. Cambridge Univ. Press; 2007.

8. Analitis A, De' Donato F, Scortichini M, Lanki T, Basagana X, Ballester F, et al. Synergistic Effects of Ambient Temperature and Air Pollution on Health in Europe: Results from the PHASE Project. Int J Environ Res Public Health. 2018;15(9).

9. Murray CJ, Lipfert FW. Inferring frail life expectancies in Chicago from daily fluctuations in elderly mortality. Inhalation toxicology. 2013;25(8):461-79.

10. De Sario M, Katsouyanni K, Michelozzi P. Climate change, extreme weather events, air pollution and respiratory health in Europe. The European respiratory journal : official journal of the European Society for Clinical Respiratory Physiology. 2013.

11. Ha J, Kim H, Hajat S. Effect of previous-winter mortality on the association between summer temperature and mortality in South Korea. Environ Health Perspect. 2011;119(4):542-6.

12. Guo Y, Punnasiri K, Tong S. Effects of temperature on mortality in Chiang Mai city, Thailand: a time series study. Environ Health. 2012;11:36.

13. Roberts S. Interactions between particulate air pollution and temperature in air pollution mortality time series studies. Environ Res. 2004;96(3):328-37.

14. Meng X, Zhang Y, Zhao Z, Duan X, Xu X, Kan H. Temperature modifies the acute effect of particulate air pollution on mortality in eight Chinese cities. Sci Total Environ. 2012;435-436:215-21.

15. Katsouyanni K PA, Touloumi G, Tselepidaki I, Moustris K, Asimakopoulos D, Poulopoulou G, Trichopoulos D. Evidence for interaction between air pollution and high temperature in the causation of excess mortality. Arch Environ Health. 1993;48(4):235-42.

16. Li D, Zhang R, Cui L, Chu C, Zhang H, Sun H, et al. Multiple organ injury in male C57BL/6J mice exposed to ambient particulate matter in a real-ambient PM exposure system in Shijiazhuang, China. Environ Pollut. 2019;248:874-87.

17. Cheng K, Yan E, Song Z, Li S, Zhang H, Zhang L, et al. Protective effect of resveratrol against hepatic damage induced by heat stress in a rat model is associated with the regulation of oxidative stress and inflammation. J Therm Biol. 2019;82:70-5.

18. Li D, Wang X, Liu B, Liu Y, Zeng Z, Lu L, et al. Exercises in hot and humid environment caused liver injury in a rat model. PLoS One. 2014;9(12):e111741.

19. Geng Y, Ma Q, Liu YN, Peng N, Yuan FF, Li XG, et al. Heatstroke induces liver injury via IL-1β and HMGB1-induced pyroptosis. J Hepatol. 2015;63(3):622-33.

20. Ambade A, Catalano D, Lim A, Mandrekar P. Inhibition of heat shock protein (molecular weight 90 kDa) attenuates proinflammatory cytokines and prevents lipopolysaccharide-induced liver injury in mice. Hepatology. 2012;55(5):1585-95.

21. Mizzen LA, Welch WJ. Characterization of the thermotolerant cell. I. Effects on protein synthesis activity and the regulation of heat-shock protein 70 expression. J Cell Biol. 1988;106(4):1105-16.

22. Islam A, Abraham P, Hapner CD, Andrews-Shigaki B, Deuster P, Chen Y. Heat exposure induces tissue stress in heat-intolerant, but not heat-tolerant, mice. Stress. 2013;16(2):244-53.

23. Archer AE, Von Schulze AT, Geiger PC. Exercise, heat shock proteins and insulin resistance. Philos Trans R Soc Lond B Biol Sci. 2018;373(1738).

24. Liu C, Xu X, Bai Y, Wang TY, Rao X, Wang A, et al. Air pollution-mediated susceptibility to inflammation and insulin resistance: influence of CCR2 pathways in mice. Environ Health Perspect. 2014;122(1):17-26.

25. Li R, Sun Q, Lam SM, Chen R, Zhu J, Gu W, et al. Sex-dependent effects of ambient PM(2.5) pollution on insulin sensitivity and hepatic lipid metabolism in mice. Part Fibre Toxicol. 2020;17(1):14.

26. Li R, Wang Y, Chen R, Gu W, Zhang L, Gu J, et al. Ambient fine particulate matter disrupts hepatic circadian oscillation and lipid metabolism in a mouse model. Environ Pollut. 2020;262:114179.

27. Cesarovic N, Jirkof P, Rettich A, Arras M. Implantation of radiotelemetry transmitters yielding data on ECG, heart rate, core body temperature and activity in free-moving laboratory mice. J Vis Exp. 2011(57).

28. Leon LR, Blaha MD, DuBose DA. Time course of cytokine, corticosterone, and tissue injury responses in mice during heat strain recovery. Journal of applied physiology (Bethesda, Md : 1985). 2006;100(4):1400-9.

29. Leon LR, DuBose DA, Mason CW. Heat stress induces a biphasic thermoregulatory response in mice. American journal of physiology Regulatory, integrative and comparative physiology. 2005;288(1):R197-204.

30. Liu Z, Li B, Tong H, Tang Y, Xu Q, Guo J, et al. Pathological changes in lung and brain during heat stress. World J Emerg Med. 2011;2(1):50-3.

31. Jain SK, Croad JL, Velusamy T, Rains JL, Bull R. Chromium dinicocysteinate supplementation can lower blood glucose, CRP, MCP-1, ICAM-1, creatinine, apparently mediated by elevated blood vitamin C and adiponectin and inhibition of NFkappaB, Akt, and Glut-2 in livers of zucker diabetic fatty rats. Mol Nutr Food Res. 2010;54(9):1371-80.

32. Hagiwara A, Cornu M, Cybulski N, Polak P, Betz C, Trapani F, et al. Hepatic mTORC2 activates glycolysis and lipogenesis through Akt, glucokinase, and SREBP1c. Cell Metab. 2012;15(5):725-38.

33. Mayer MP, Bukau B. Hsp70 chaperones: cellular functions and molecular mechanism. Cell Mol Life Sci. 2005;62(6):670-84.

34. Cong X, Zhang Q, Li H, Jiang Z, Cao R, Gao S, et al. Puerarin ameliorates heat stress-induced oxidative damage and apoptosis in bovine Sertoli cells by suppressing ROS production and upregulating Hsp72 expression. Theriogenology. 2017;88:215-27.

35. Leon LR, Helwig BG. Heat stroke: role of the systemic inflammatory response. J Appl Physiol (1985). 2010;109(6):1980-8.

36. Hensen SM, Heldens L, van Enckevort CM, van Genesen ST, Pruijn GJ, Lubsen NH. Activation of the antioxidant response in methionine deprived human cells results in an HSF1-independent increase in HSPA1A mRNA levels. Biochimie. 2013;95(6):1245-51.

37. Choudhury A, Bullock D, Lim A, Argemi J, Orning P, Lien E, et al. Inhibition of HSP90 and Activation of HSF1 Diminish Macrophage NLRP3 Inflammasome Activity in Alcohol-Associated Liver Injury. Alcohol Clin Exp Res. 2020;44(6):1300-11.

38. Goto A, Egawa T, Sakon I, Oshima R, Ito K, Serizawa Y, et al. Heat stress acutely activates insulin-independent glucose transport and 5'-AMP-activated protein kinase prior to an increase in HSP72 protein in rat skeletal muscle. Physiol Rep. 2015;3(11).

39. Kitano S, Kondo T, Matsuyama R, Ono K, Goto R, Takaki Y, et al. Impact of hepatic HSP72 on insulin signaling. Am J Physiol Endocrinol Metab. 2019;316(2):E305-e18.

40. Drew BG, Ribas V, Le JA, Henstridge DC, Phun J, Zhou Z, et al. HSP72 is a mitochondrial stress sensor critical for Parkin action, oxidative metabolism, and insulin sensitivity in skeletal muscle. Diabetes. 2014;63(5):1488-505.

41. Thorens B. GLUT2, glucose sensing and glucose homeostasis. Diabetologia. 2015;58(2):221-32.

42. Li L, Yao Y, Zhao J, Cao J, Ma H. Dehydroepiandrosterone protects against hepatic glycolipid metabolic disorder and insulin resistance induced by high fat via activation of AMPK-PGC-1α-NRF-1 and IRS1-AKT-GLUT2 signaling pathways. Int J Obes (Lond). 2020;44(5):1075-86.

43. Petersen MC, Shulman GI. Mechanisms of Insulin Action and Insulin Resistance. Physiol Rev. 2018;98(4):2133-223.

44. Xu X, Liu C, Xu Z, Tzan K, Zhong M, Wang A, et al. Long-term exposure to ambient fine particulate pollution induces insulin resistance and mitochondrial alteration in adipose tissue. Toxicol Sci. 2011;124(1):88-98.

45. Tilg H, Moschen AR. Inflammatory mechanisms in the regulation of insulin resistance. Mol Med. 2008;14(3-4):222-31.

46. Wieser V, Moschen AR, Tilg H. Inflammation, cytokines and insulin resistance: a clinical perspective. Arch Immunol Ther Exp (Warsz). 2013;61(2):119-25.

47. Xu J, Zhang W, Lu Z, Zhang F, Ding W. Airborne PM(2.5)-Induced Hepatic Insulin Resistance by Nrf2/JNK-Mediated Signaling Pathway. Int J Environ Res Public Health. 2017;14(7).

48. Zhao C, Niu M, Song S, Li J, Su Z, Wang Y, et al. Serum metabolomics analysis of mice that received repeated airway exposure to a water-soluble PM2.5 extract. Ecotoxicol Environ Saf. 2019;168:102-9.

49. Wang R, Han X, Pang H, Hu Z, Shi C. Illuminating a time-response mechanism in mice liver after PM(2.5) exposure using metabolomics analysis. Sci Total Environ. 2021;767:144485.

Tables

Table 1. Primers used for real-time PCR

Gene	Forward primer	Reverse primer
IL-1β	CCTTCCAGGATGAGGACATGA	AACGTCACACACCAGCAGGTT
IL-6	TCCAGTTGCCTTCTTGGGAC	GTGTAATTAAGCCTCCGACTTG
TNF-α	CATCTTCTCAAAATTCGAGTGACAA	TGGGAGTAGACAAGGTACAACCC
HSF1	AAGCTGTGGACCCTCGTGA	GGGCCTCGTTCTCGTGCTT
Hspa1a	TGGTGCAGTCCGACATGAAG	CACGTTTAGACCGGCGATCA
Slc2a2	ATGACCGGAAAGCTGCCATT	GAGTGTGGTTGGAGCGATCT
β-actin	TGTGATGGTGGGAATGGGTCAGAA	TGTGGTGCCAGATCTTCTCCATGT

Table 2. Elemental composition of $PM_{2.5}$ collected in FA and PM chambers

Elements	FA chamber, ng/mg		PM chamber, ng/mg	
	Mean	SEM	Mean	SEM
Na	6.74	0.14	50.15	0.87
Mg	7.94	1.24	49.90	2.82
Si	5.36	0.68	68.51	4.15
S	17.76	1.18	178.18	6.42
K	23.62	4.49	186.00	6.39
Ca	15.30	3.56	164.85	7.21
Ti	1.31	0.13	20.33	1.04
Mn	2.22	0.27	29.80	1.42
Fe	11.18	0.90	149.48	5.51
Ni	1.26	0.09	16.73	0.63
Cu	2.10	0.08	25.19	1.09
Zn	3.66	0.19	40.74	1.37
Sr	0.95	0.05	8.28	0.18
Y	0.06	0.09	1.00	0.24

Figures

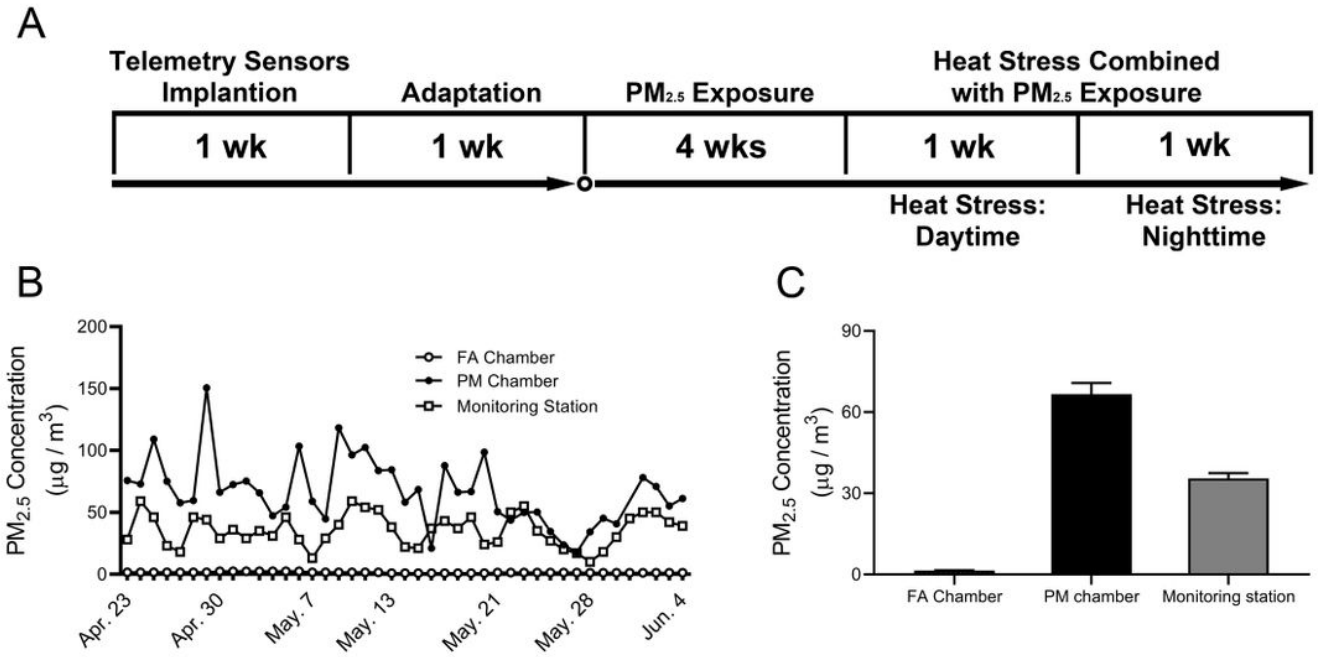

Figure 1

Experimental schedule and PM2.5 concentrations during the exposure period. A, Experimental schedule of heat stress combined with PM2.5 exposure in this study. B, PM2.5 concentrations in the FA chamber, PM chamber and ambient air from the monitoring station during the exposure period. C, Bar graph of mean daily PM2.5 concentrations in the FA chamber, PM chamber and ambient air from the monitoring station during the exposure period.

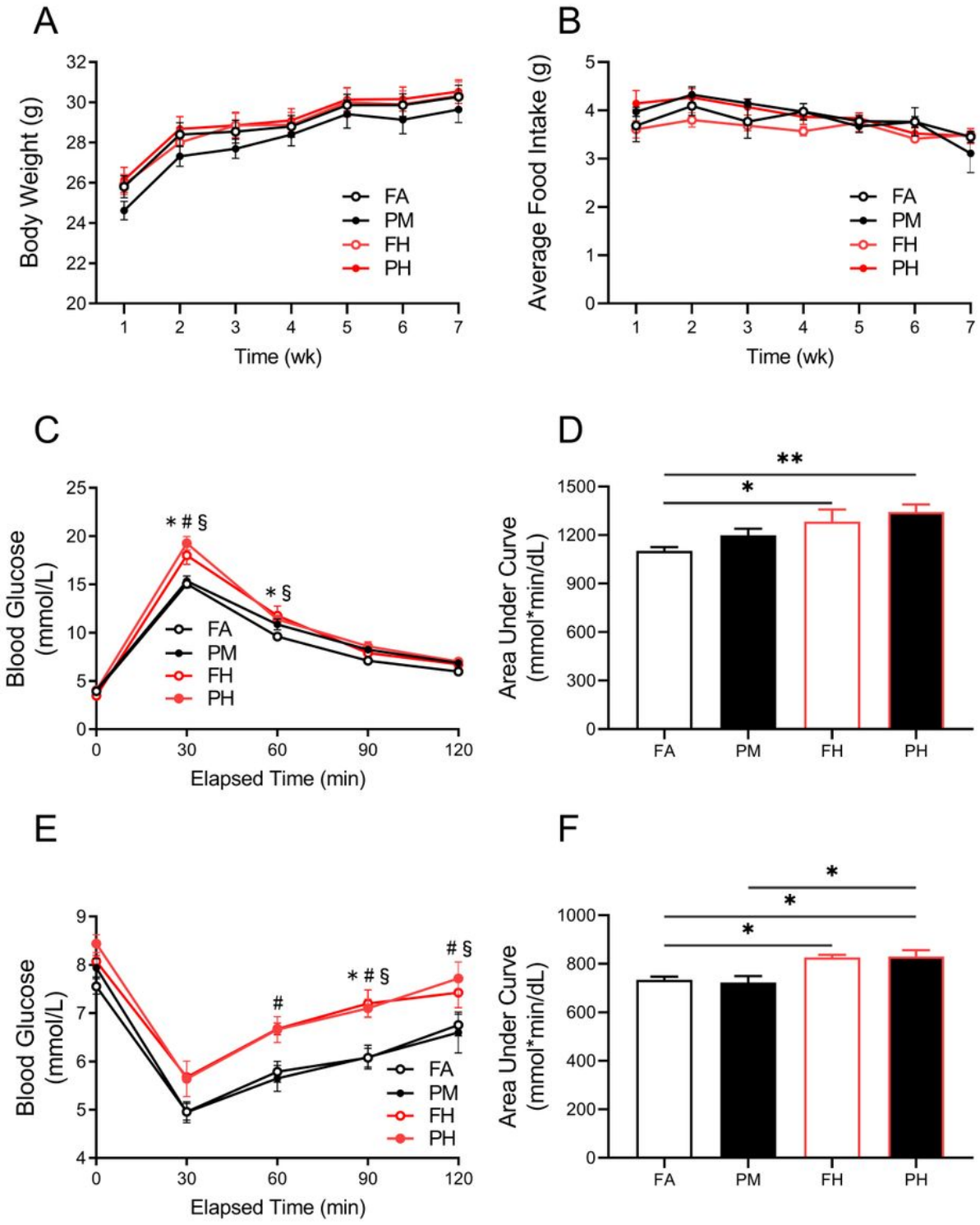

Figure 2

Metabolic characteristics of mice in response to heat stress combined with PM2.5 exposure A-B, Weekly body weight and average food intake during the exposure period. C-D, GTT and GTT analysis with AUC. E-F ITT and ITT analysis with AUC. In C and E, * $P < 0.05$ when FH compared to FA group; # $P < 0.05$ when PH compared to PM group; § $P < 0.05$ when PH compared to FA group. In D and F, * $P < 0.05$; ** $P < 0.01$. n = 12-14.

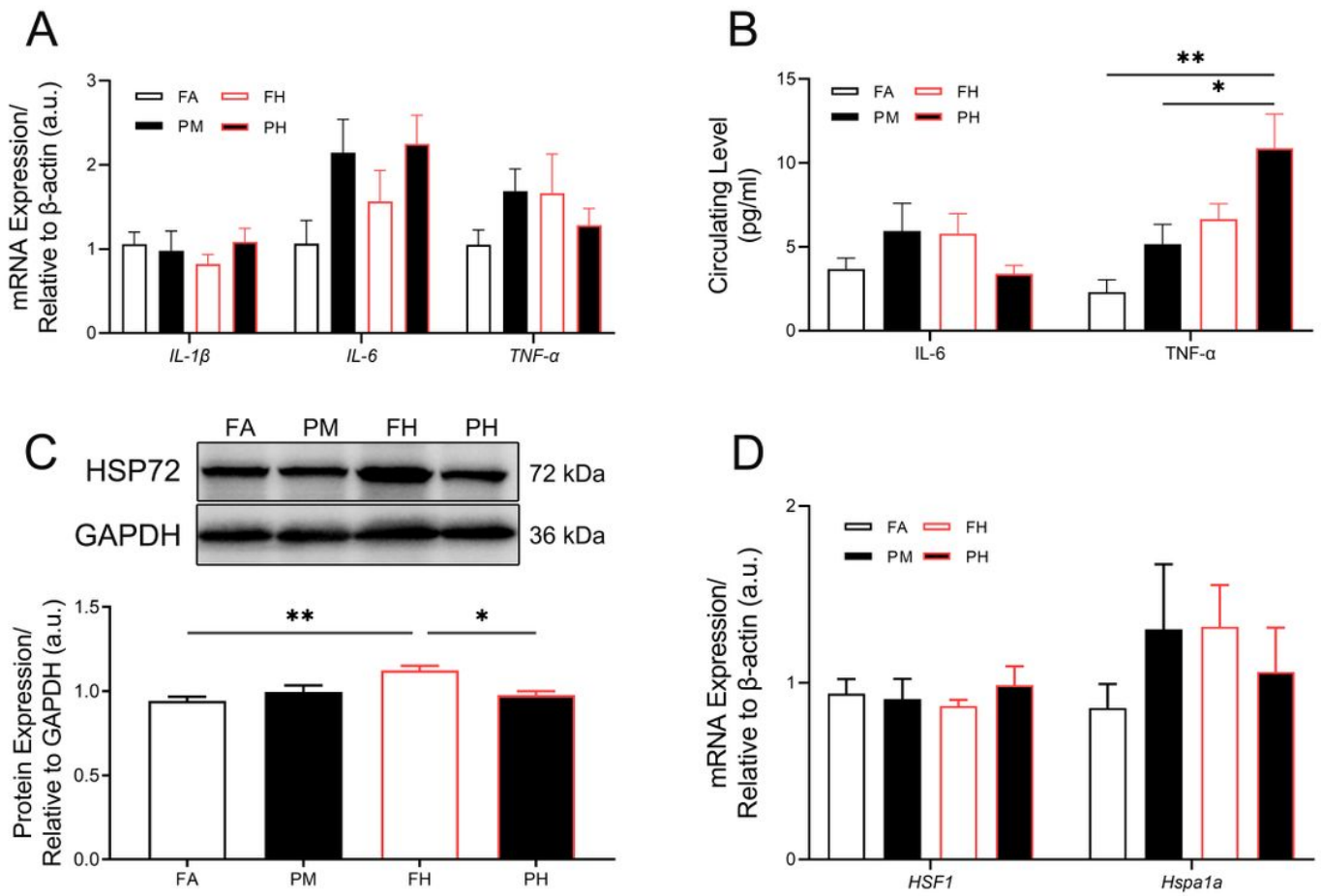

Figure 3

Circulating cytokines and hepatic expression of HSP72 in response to heat stress combined with PM2.5 exposure. A, mRNA levels of IL-1β, IL-6, and TNF-α in the liver. B, Circulating levels of IL-6 and TNF-α. C, mRNA levels of HSF1 and Hspa1a in the liver. D, Representative bands and analyzed protein levels of HSP72 in the liver at the end of the exposure. * $P < 0.05$; ** $P < 0.01$. n = 5-6.

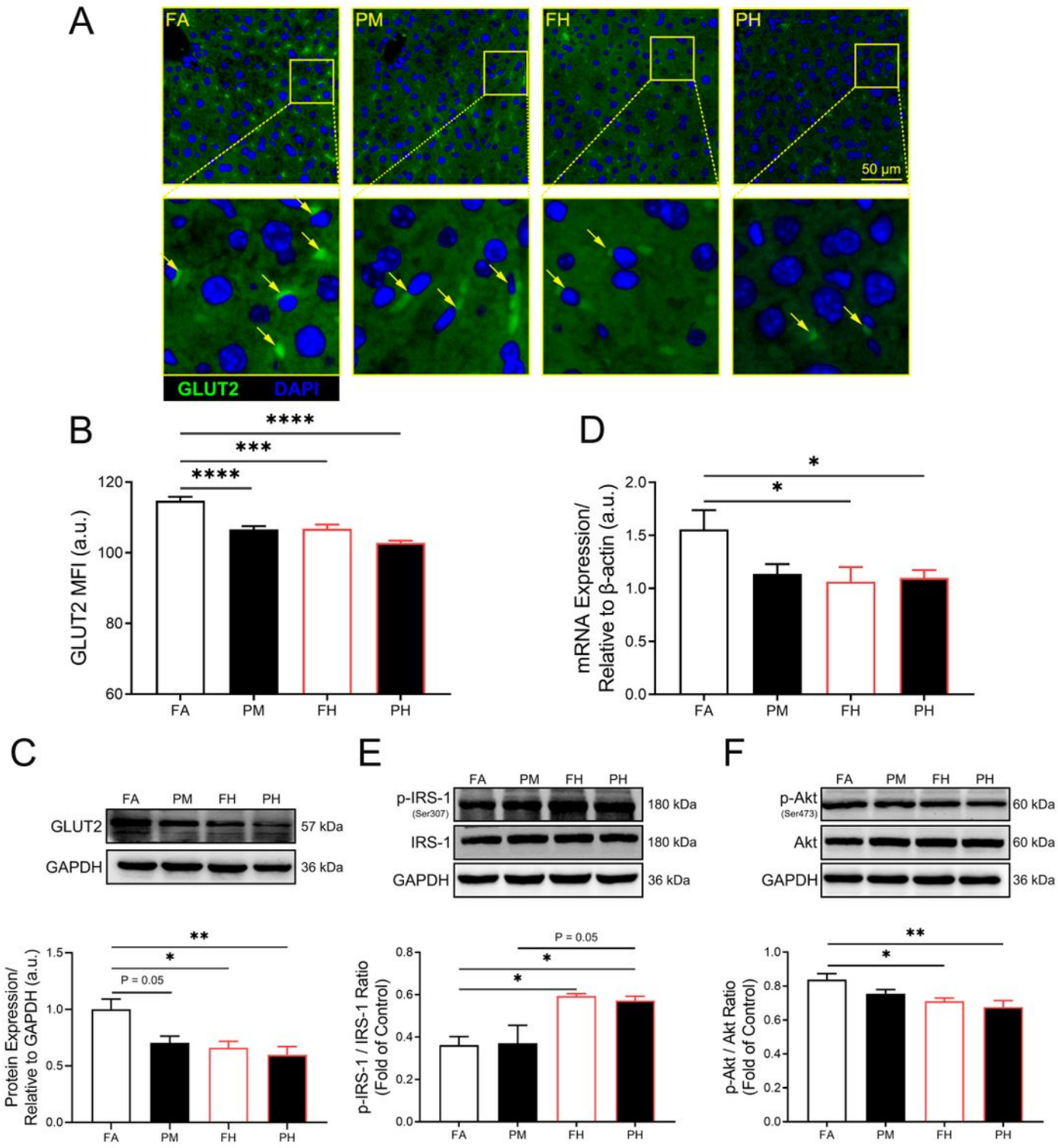

Figure 4

Hepatic GLUT2 expression and insulin signaling in response to heat stress combined with PM2.5 exposure. A, Immunofluorescence staining for GLUT2 (green and arrows) and DAPI (blue) in the liver after 6 weeks of exposure in FA, PM, FH, and PH groups. Images were obtained under the same conditions at a magnification of 200× across treatment groups. Scale bar, 50 μm. B, Quantitative analysis of the MFI of GLUT2 protein by immunofluorescence assay. C, Representative bands and analyzed protein levels of

GLUT2. D, mRNA levels of Slc2a2 in liver. E-F, Representative bands and analyzed protein levels of p-IRS-1Ser307 and p-AktSer473 in the liver at the end of heat stress combined with PM2.5 exposure. * P < 0.05; ** P < 0.01; *** P < 0.001; **** P < 0.0001. n = 5-6.

Supplementary Files

This is a list of supplementary files associated with this preprint. Click to download.

- Sup1.tif
- Sup2.tif